PHYSICAL REVIEW A VOLUME 43, NUMBER 10 15 MAY 1991

Cluster-collision frequency. II. Estimation of the collision rate

A. S. Amadon and W. H. Marlow*
Department of Nuclear Engineering, Texas A&M University, College Station, Texas 77843-3133

(Received 24 September 1990)

Gas-phase cluster-collision rates, including effects of cluster morphology and long-range intermolecular forces, are calculated. Identical pairs of icosahedral or dodecahedral carbon tetrachloride clusters of 13, 33, and 55 molecules in two different relative orientations were discussed in the preceding paper [Phys. Rev. A **43**, 5483 (1991)]: long-range interaction energies were derived based upon (i) exact calculations of the iterated, or many-body, induced-dipole interaction energies for the clusters in two fixed relative orientations; and (ii) bulk, or continuum descriptions (Lifshitz–van der Waals theory), of spheres of corresponding masses and diameters. In this paper, collision rates are calculated according to an exact description of the rates for small spheres interacting via realistic potentials. Utilizing the interaction energies of the preceding paper, several estimates of the collision rates are given by treating the discrete clusters in fixed relative orientations, by computing rotationally averaged potentials for the discrete clusters, and by approximating the clusters as continuum spheres. For the discrete, highly symmetric clusters treated here, the rates using the rotationally averaged potentials closely approximate the fixed-orientation rates and the values of the intercluster potentials for cluster surface separations under 2 Å have negligible effect on the overall collision rates. While the 13-molecule cluster-collision rate differs by 50% from the rate calculated as if the cluster were bulk matter, the two larger cluster-collision rates differ by less than 15% from the macroscopic rates, thereby indicating the transition of microscopic to macroscopic behavior.

I. INTRODUCTION

Collisions of clusters in the gas phase are responsible through different mechanisms for cluster formation via homogeneous or critical nucleation and for the evolution of the size distribution of stable clusters. Since critical nucleation is generally assumed to be an equilibrium process dominated by the interaction of the condensing vapor with the evanescent, subcritical clusters, its kinetic description may be formulated in terms of microscopic reversibility.[1] In contrast, when thermodynamically stable clusters are present, the environment is such that the elementary condensing vapor species does not necessarily dominate growth because of its prior depletion.[2] For this situation, the cluster-cluster collisions that dominate the cluster-size-distribution evolution are *effectively* irreversible because the large number of vibrational modes of the cluster system dissipate, or thermalize, the collisional energy.[3] This second case, collisions of stable clusters, is the subject treated in this and the preceding paper,[4] henceforth referred to as paper I.

As argued in paper I, a factoring of the cluster reaction rate into the collision rate and the reaction probability can normally be made and should always be possible for chemically similar clusters.[5] Therefore, the collision rate, or collision frequency, is generally the upper limit for the overall reaction.[6] Since the "reaction" of sticking or adhesion between colliding clusters is highly favored in innumerable cases of interest for both research and applications, the collision frequency is also the reaction rate. The objective of these papers is to contribute to the development of methods for computing collision rates that are both computationally tractable and physically meaningful. Based upon these rates, computations for the cluster-size-distribution evolution needed in a variety of applications can then be made.

In general, the collisions of clusters are subject to questions similar to those which apply to molecular collisions. The contributions of the different relative orientations of the colliding clusters at contact determine the overall geometrical collision cross section, and the orientation-dependent long-range interactions between the clusters give the enhancement of the collision rate beyond that arising from geometry alone. While the exact treatment of these questions is too complex for the calculation of the large number of rates that enter computations of size-distribution evolution, it may not be required. Unlike molecular collisions where reactions are determined by the details of the approach to collision, for collisions of stable clusters this detail is often unnecessary, as argued above and in paper I. For these reasons, the paradigm of detailed molecular-collision calculations may not be a useful starting point for constructing a computational approach to the estimation of cluster-collision rates.

Ultrafine particulate matter in the gas phase, or free-molecular aerosols, provide an alternative paradigm for the construction of cluster-collision rates. There, particles are customarily approximated as spheres, except in the most extreme cases, and a rigorous formulation exists of the effect on collisions of realistic long-range forces between electrically neutral, free-molecular regime particles (radius much smaller than the mean free path of background gas).[7] The benefits of this approach are that "large" clusters are indistinguishable in overall dimensions from ultrafine particles and that the collision theory with recent extensions[8] is entirely consistent with molecular-collision theory.

In this paper an approach for estimating the collision rates of clusters is developed which is based upon the results for free-molecular spheres. The effects of shape and relative orientation are taken into account by approximating the upper and lower limits of the rates based upon appropriate rates for corresponding spheres, and the results are compared with rates for compositionally equivalent macroscopic spheres and shown to converge to those rates for sufficiently large clusters.

II. COLLISION FREQUENCY

A. Spherical aerosol particles

Aerosols frequently are comprised of particles that are spherical due either to their composition or formation processes. For the calculation of the collision frequency Φ_{AB} of condensed-phase particles, if λ_g/r_A and $\lambda_g/r_B>10$, where λ_g and $r_{A,B}$ are the mean free path of background gas molecules and A,B-particle radii, respectively, $|\Delta E(\lambda_g)|/kT \ll 1$, and the interaction potential of particles A and B at center-of-mass separation R $\Delta E(R)\rightarrow -\infty$ for $R\rightarrow r_A+r_B$ then a rigorous, analytic formula for the collision rate is available.[7] In the equations listed above, k is the Boltzmann constant and T is the temperature of the system. If the long-range interaction potential energy is calculated either according to the sum over London–van der Waals pair interactions or according to the continuum Lifshitz theory of the van der Waals interaction,[9] the potentials obey these limiting conditions. While the limiting form is unphysical for sufficiently small separations, the integrals in the exact collision formula converge for separations well beyond the orbital overlap region where these macroscopic potentials are still useful.[10]

For a pair of clusters, the fact that their interaction energy ΔE is bounded as they approach, as treated in Paper I, makes the utilization of the aerosol collision-rate formula[7] questionable for the computation of cluster collisions, even when the clusters are treated as spherical. Recently, this deficiency has been addressed[8] by generalizing the earlier work with the result that the collision frequency for free-molecular aerosol particles interacting via a monotonic, attractive potential is given by

$$\Phi^{(\mathrm{FM})}(\Delta E)=\pi v_{\mathrm{av}}(r_A+r_B)^2\exp\left[-\left[\frac{\Delta E(\sigma_1)}{kT}+\frac{\sigma_1}{2kT}\frac{d\Delta E(r)}{dr}\bigg|_{\sigma_1}\right]\right]-\frac{\pi v_{\mathrm{av}}}{2kT}\int_{\sigma_1}^{\infty}d\sigma\left[\frac{d\Delta E(\sigma)}{d\sigma}+\sigma\frac{d^2\Delta E(\sigma)}{d\sigma^2}\right]\sigma^2\exp\left[-\frac{1}{kT}\left[\frac{\sigma}{2}\frac{d\Delta E(\sigma)}{d\sigma}+\Delta E(\sigma)\right]\right]\ , \tag{1}$$

with the subsidiary condition

$$\frac{\sigma}{2}\left[\frac{d\Delta E}{dr}\right]_{\sigma}\left[\left[\frac{\sigma}{r_A+r_B}\right]^2-1\right]+\Delta E(r_A+r_B)-\Delta E(\sigma)=0\ , \tag{2}$$

where $v_{\mathrm{av}}=\sqrt{8kT/\pi\mu}$ and μ is the reduced mass of the particles. σ_1 in Eq. (1) is given as follows: If there exists a $\sigma_0>(r_A+r_B)$ that is a root of Eq. (2), then $\sigma_1=\sigma_0$; otherwise, $\sigma_1=r_A+r_B$. For a potential that goes to minus infinity at contact such as for particles treated as condensed matter, there is always a $\sigma>(r_A+r_B)$ that satisfies Eq. (2) and in this limiting case of a singular attractive contact potential, the first term in Eq. (1) goes to zero.[7]

The literature contains several computationally simpler alternatives to Eq. (2) which are based upon different approximations and whose results will be calculated below for the purpose of completeness. In the simplest case, if the two particles are assumed to have no long-range interaction potential, their collision rate is the hard-sphere rate

$$\Phi^0=\pi v_{\mathrm{av}}(r_A+r_B)^2\ , \tag{3}$$

where quantity $\pi(r_A+r_B)^2$ is the hard-sphere cross section.

If the long-range attraction forces are considered, the collision frequency is multiplied by a correction factor Ψ, called the *collision-rate enhancement factor* (CREF). As a result, the physical collision frequency Φ is given by the product $\Psi\Phi^0$. If this expression is rewritten as

$$\Phi=\pi b_m^2 v_{\mathrm{av}}\ , \tag{4}$$

then b_m is the capture radius or maximum impact parameter leading to collision.

The analysis of particle trajectories before and after encounter in the center-of-mass system leads to a simple correlation between the impact parameter b and the distance of closest approach or turning point R_m:

$$b^2=R_m^2\left[1-\frac{\Delta E(R_m)}{E_0}\right]. \tag{5}$$

Here, E_0 is the initial total translational kinetic energy of the particles in the center-of-mass system (i.e., the kinetic energy of the reduced mass at large separations). According to the Fuchs-Sutugin approximation,[11] $E_0=\frac{3}{2}kT$ and for attractive potentials, the condition $(db^2/dR_m)=0$ determines R_m so that the square of the capture radius in Fuchs' approximation is

$$b_m^{(\mathrm{F})2}=R_m^2\left[1-\frac{2\Delta E(R_m)}{3kT}\right]. \tag{6}$$

Recently, Sceats[12,13] used a different approach for the problem. He based his approximation on a thermal average of the angular or centrifugal part of the kinetic energy. The resulting average effective potential, the interaction potential plus the angular part of the kinetic energy, that he used has the form

$$\langle V_{\text{eff}}\rangle(R)=\Delta E(R)-2kT\ln(R/R_0)\ ,$$

where R_0 is a constant. By determining the maximum for this effective potential, located at $R=R_T$, Sceats finds the following formula for the capture radius:

$$b_m^{(\mathrm{S})^2}=R_T^2\exp\left[\frac{-\Delta E(R_T)}{kT}\right]\ , \tag{7}$$

where R_T is determined by $d(\langle V_{\text{eff}}\rangle)/dR=0$ or, equivalently,

$$R_T(d\Delta E/dR)_{R_T}-2kT=0\ .$$

Of the formulas presented here, only Eq. (1) sums over all trajectories to give the realistic weighting of the collisions dependent upon their incident kinetic energies distributed according to the Maxwell distribution.

B. Intercluster potential energies and cluster parameters

For computing the long-range interaction potentials ΔE needed in collision calculations, the following interrelated questions should be addressed: (1) For clusters of discrete molecules with specific geometry, what is the correct form of the potential? (2) How does that potential converge with increasing cluster size to the corresponding potential for condensed matter or matter in the continuum approximation? (3) How can the cluster interaction energies or collision rates be averaged over geometry or relative orientation to produce rates that can be compared with compositionally equivalent macroscopic spheres? (4) What are the practical effects on the calculated collision rates of the difference between the discrete and continuum energies? (5) Can limiting cases of the cluster-collision frequencies be given which bracket the true value? In paper I the first two of these questions are treated while the last three are the subjects of the present paper, which applies the results of the energy calculations to collision-frequency estimation.

Clusters of carbon tetrachloride molecules are treated in these papers. This choice was made for the following reasons: (1) Extensive spectroscopic data required for computation of interaction energies are available; (2) as a closed-shell molecular species, its interaction-energy characteristics in discrete cluster and continuum pictures and the results of computations based upon them should be broadly relevant; and (3) the molecule can be reasonably treated as if it were spherical, which allows the construction of clusters based upon this elementary unit. In paper I the interaction energies of pairs of identical clusters have been computed as functions of separation for 13-, 33-, and 55-molecule clusters. The largest and smallest clusters are icosahedrons and the others are dodecahedrons; all structures are relaxed to local minimal-energy configurations under the influence of the intermolecular potential used here. Repulsive, pairwise, short-range potentials between molecules are used to ensure realistic intermolecular separations while attractive interactions arise from the induced-dipole interaction iterated over all molecules (treated as Drude oscillators) of the two clusters, a potential which generalizes the classical London–van der Waals intermolecular potential between a pair of molecules and is consistent with the Lifshitz–van der Waals potential between matter in the continuum picture.

Two relative orientations are selected for each cluster pair with energies computed at a range of separations for each orientation. The orientations chosen are those corresponding to the maximum and minimum separations of centers of mass when the clusters are in contact. For both the icosahedral pairs and the dodecahedral pair, the clusters are mirror images of each other along the threefold and the fivefold axes of symmetry. In the case of the dodecahedron, the fivefold symmetric orientation provides the closest approach for the centers of mass while for the icosahedrons the threefold symmetric orientation provides this minimum distance. The radius of a cluster is defined as half the center-of-mass separation at closest approach. Thus, actual variations in cluster dimensions and interaction energies that are associated with different relative orientations are taken into account.

For the purpose of defining condensed-phase particles that correspond to the clusters, the radii of the particles initially are taken to be radii of the spheres circumscribed about the clusters; these radii are the larger of the two radii defined above for each cluster. The interaction energy of a pair of particles is then computed according to the standard formula which sums over pair interactions with the Lifshitz-Hamaker constant dependent upon the mass of the individual cluster in order that the comparison be meaningful. Collision rates then follow from utilization of this energy in Eq. (1) where the first term vanishes due to the unbounded potential characteristic of continuum interaction energies at particle contact.

The potentials calculated for the discrete clusters are all finite at contact, but their lack of spherical symmetry requires either that averaging procedures be introduced or that special interpretations be conferred upon the procedures selected for calculating the rates. Both of these approaches were followed in paper I.

(1) In the first procedure, the energies themselves were averaged by weighting their values according to the degeneracy of each relative orientation,

$$\Delta E_{\text{av}}=(20\Delta E_{\text{threefold}}+12\Delta E_{\text{fivefold}})/32\ .$$

This average energy is then used in Eq. (1) to compute a rate denoted $\mathcal{R}_{\text{av}}^n$, where n is the number of molecules in each of the two interacting clusters.

(2) The second procedure treats each cluster orientation alone. The potential as a function solely of separation for each relative orientation of the clusters is utilized as the basis for computing the collision frequency according to Eq. (1), thereby reducing the computation to the problem of two spheres with radii appropriate to the par-

ticular orientation as already described. As a result, two collision frequencies are computed and since they are derived from the geometrical limiting cases of maximum and minimum distances from the center of mass to the surface, or maximum and minimum collision radii, they are assumed to give limiting values for the true collision frequency.

C. Calculational results

The energies derived in paper I were used to compute collision frequencies according to the models discussed above. Due to the complexity of the interaction potential-energy calculations, evaluations were made on sets of discrete points and seventh-order splines were fit to the computed values to give energy curves with continuous first and second derivatives.

A critical question for the evaluation of cluster-collision frequencies is the detail required in the intercluster potential. If significant contributions are made to Eq. (1) for values of the argument σ that are close to the overlap region of the clusters' surface molecules, then the potentials used for collision-frequency calculations will require the corresponding level of detail whether that be via phenomenological r^{-m} potentials as used here or through solution of the appropriate wave equations for the electrons of the cluster. This question is answered through the evaluation of the integrand of Eq. (1) given in Fig. 1. In these graphs the integrands are given for energies based on the two orientations of the clusters, for energies derived from the weighted average of the energies for these two orientations, and for energies based upon the continuum models for the clusters. The significant quantities are the minimum values for the center-of-mass separation distances where the curves depart from the axes. In all cases, those distances correspond to cluster surface-to-surface separations comparable to or greater than 2 Å. The cluster diameters used to interpret these graphs are given in Table I (denoted d_{clust}, which is the apparent diameter for the cluster pair, defined as the center-of-mass separation of clusters at minimum separation) as discussed above and in paper I. Thus, for the purpose of collision-frequency calculations, only the long-range tail of the complete intercluster potential enters. This result corroborates the validity of factoring the reaction rate into collision-frequency and reaction-probability terms.

The values of the collision frequencies (or fluxes), capture radii, and CREF's computed from both the Lifshitz-Hamaker approximation and the discrete intermolecular potentials are given in Table I. The abbreviation LH stands for the Lifshitz-Hamaker potential utilized for the condensed-matter interaction. Results are given for the full calculation according to Eq. (1), for the Fuchs-Sutugin approximation following from Eq. (6), and for Sceats's approximation following from Eq. (7). In all cases the two approximations give lower fluxes than the full calculation and are included for completeness but will not be discussed further.

In Table I the Eq. (1) flux consists of the two components in Eq. (1) unlike the older result[7] derived for

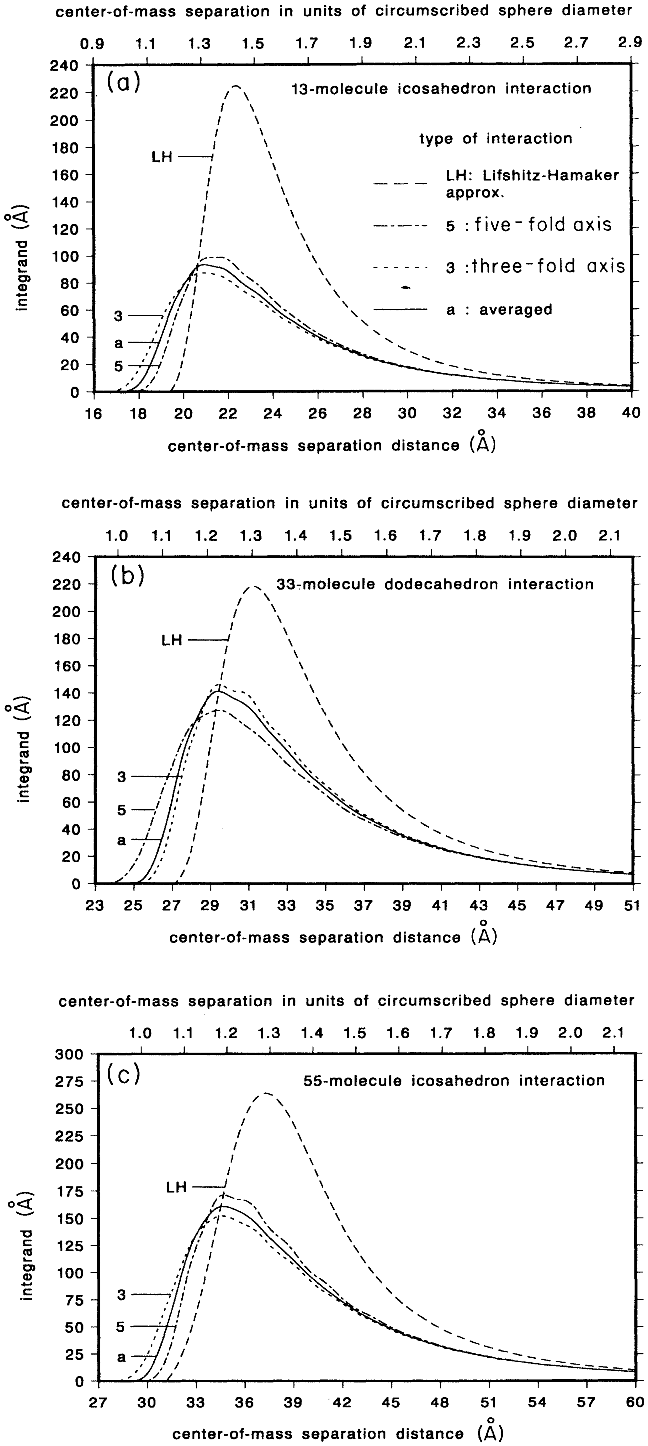

FIG. 1. (a) Integrand in collision-rate integral, Eq. (1), as a function of center-of-mass separation distance between interacting carbon tetrachloride clusters for different forms of the intercluster potential: Lifshitz-Hamaker approximation models clusters as bulk-matter sphere; fivefold axis and threefold axis for discrete clusters in mirror-symmetric orientation along respective axis; averaged or rotationally averaged discrete energies. 13-molecule icosahedron. (b) Same as above for 33-molecule dodecahedron. (c) Same as above for 55-molecule icosahedron.

TABLE I. Collision frequencies and derived parameters from alternative methods.

	13-molecule cluster				33-molecule cluster				55-molecule cluster			
	Symmetry		Average		Symmetry		Average		Symmetry		Average	
	Threefold	Fivefold	energy	LH	Fivefold	Threefold	energy	LH	Threefold	Fivefold	energy	LH
Interaction type												
d_{clust} (Å)	14.71	17.02	17.02	17.02	20.25	23.99	23.99	23.99	23.77	28.21	28.21	28.21
Equation (1)												
$\Phi(10^{-10}\text{cm}^3/\text{sec})$	18.01	18.23	18.11	32.19	21.62	21.87	21.74	28.24	23.42	23.59	23.40	32.93
Capture radius (Å)	26.98	27.15	27.05	36.07	37.31	37.53	37.41	42.64	44.12	44.28	44.10	52.32
CREF	3.365	2.544	2.527	4.491	3.395	2.447	2.432	3.159	3.444	2.464	2.444	3.440
Fuchs												
$\Phi(10^{-10}\text{cm}^3/\text{sec})$	13.08	13.59	13.30	14.89	15.92	16.51	16.32	17.91	17.29	17.78	17.50	19.35
Capture radius (Å)	22.99	23.44	23.19	24.53	32.02	32.61	32.42	33.96	37.91	38.44	38.13	40.10
CREF	2.444	1.896	1.856	2.077	2.50	1.847	1.826	2.003	2.543	1.857	1.827	2.021
Sceats												
$\Phi(10^{-10}\text{cm}^3/\text{sec})$	15.03	15.41	15.18	16.57	18.17	18.61	18.46	19.86	19.71	20.05	19.85	21.49
Capture radius (Å)	24.65	24.95	24.77	25.88	34.21	34.61	34.47	35.76	40.47	40.83	40.61	42.27
CREF	2.808	2.150	2.119	2.312	2.853	2.081	2.065	2.222	2.898	2.094	2.073	2.245

singular, attractive contact potentials where the first term was not present. The calculations showed that in all cases the new term made a negligible contribution to the overall flux, never exceeding 0.05% of the final value. Thus, the nonintegral first term in Eq. (1), which is the term that has a direct dependence on d_{clust}, can be dropped in practice and the dependence on the physical radius is weakened. The effect of this weakened dependence is seen in the collision fluxes or capture radii which differ by less than 1% for the two distinct orientations for which the discrete intercluster potentials were evaluated for each size of cluster. Thus, at least for these highly symmetric clusters, the collision fluxes or frequencies are similar regardless of the mutual orientations upon which the interaction potentials were based, a result that is also manifested by the close agreement with the results calculated from the averaged discrete intercluster potentials.

The CREF's, Ψ, for the rates corresponding to the two specific orientations differ by as much as 40% in the three cases examined here. This is due to their strong dependence on the center-of-mass distance at contact, $\Psi=(b_m/d_{\text{clust}})^2$, which did not exist for the flux or capture radius calculations. Indeed, this discrepancy between the CREF's of the same interaction case is directly dependent on the square of the ratio of the associated minimum and maximum contact separations d_{clust}. This ratio is more pronounced for the 33-molecule dodecahedron and the 55-molecule icosahedron than for the 13-molecule icosahedron and accounts therefore for the enhanced gap between the limiting-case potential CREF's for the two larger clusters.

In Table I the CREF's corresponding to the rotationally averaged potentials are computed with d_{clust} equal to the circumscribed sphere diameters. Since these values do not reflect the real average center-of-mass separations at contact, the corresponding enhancements differ significantly from the ranges given by the discrete cluster calculations.

For the CREF's arising from the continuum-model approach, no dependence on contact separation is present. This well-known result is due to the scaling property of the long-range force[14] when retardation is neglected.[15] For this reason, dependence upon d_{clust} in this case only occurs through the capture radius ($b_m^2=\Psi d_{\text{clust}}^2$).

The dimensions of the molecules comprising the bulk-matter particles are not negligible compared to the particle diameters. Therefore, the collision frequencies, or capture radii, calculated with d_{clust} equal to the cluster circumscribed sphere diameters, are inconsistent with the values found from the microscopic model as described above. The fractional deviations of the collision rates for the continuum model from the discrete cluster rates are 75%, 30%, and 40%, respectively, for the 13-, 33-, and 55-molecule clusters. The fall from 75% to 40% for the icosahedral structures tends to reflect the expected convergence of the molecular-based model for large clusters to the macroscopic approximation. The smaller 30% deviation indicates that the dodecahedron is closer to a sphere than the icosahedron, corresponding to the fact that the dodecahedron has more vertex molecules (20) in contact with its circumscribed sphere than the icosahedron (12).

An averaged d_{clust} can be computed in exactly the same way that the averaged potential was computed by weighting the different d_{clust} according to the frequency of occurrence of the different axes of interaction. Thus,

$$\langle d_{\text{clust}}\rangle=\frac{12(d_{\text{clust}})_{\text{fivefold}}+20(d_{\text{clust}})_{\text{threefold}}}{32}\ . \tag{8}$$

Here, the subscripts correspond to the respective axes of symmetry along which the molecular interactions are computed for each pair of clusters. This new value leads to new CREF's for the rotationally averaged potentials that can be compared with the CREF's for the continu-

TABLE II. Collision parameters based on corrected contact separation, $\langle d_{\text{clust}} \rangle$ using Eq. (1): values reproduced from Table I. Parameters obtained from corrected values appear with an asterisk.

	13-molecule cluster		33-molecule cluster		55-molecule cluster	
Interaction model	Average energy	LH	Average energy	LH	Average energy	LH
$\langle d_{\text{clust}} \rangle$ (Å)	15.58*		22.59*		25.44*	
Φ (10^{-10} cm^3/sec)	18.11	26.96*	21.74	25.03*	23.40	26.78*
Capture radius (Å)	27.05	33.01*	37.41	40.15*	44.10	47.18*
CREF	3.061*	4.491	2.743*	3.159	3.006*	3.440

um spheres. Conversely, those averaged contact separations can be used in the macroscopic model to yield new collision rates and capture radii.

The collision parameters obtained from this approach of using $\langle d_{\text{clust}} \rangle$ are presented in Table II; the new corrected values appear with an asterisk and the values reproduced from Table I are also given. From these results, a more coherent comparison between macroscopic and discrete-molecular models can be drawn. Now, the rotationally averaged potential CREF's are within the range imposed by the limiting-case potentials (see Table I). This picture corresponds more closely to the picture of a diameter that is averaged over the effective-interaction contact diameters, rather than that of the sphere circumscribing the cluster.

The new fractional deviations between the collision rates, cross sections, and CREF's based on the macroscopic approximation with those from the discrete model are, respectively, 49%, 15.1%, and 14.4% for the 13-, 33-, and 55-molecule clusters' interactions. This time a real convergence is observed as the clusters increase in size. A greater relative deviation might have been expected between the 33-molecule and 55-molecule cases, but, as mentioned above, the fact that the dodecahedral structure is closer to a sphere than the icosahedral structure accounts for the small improvement.

III. SUMMARY AND CONCLUSIONS

The collision rates, or collision frequencies, of three pairs of icosahedral or dodecahedral identical molecular clusters of increasing size have been calculated via several approaches that take into account effects of the nonspherical shape of the clusters. Intercluster potential energies given in paper I are shown to affect the collision rates primarily at cluster separations greater then 2 Å where effects of overlap of surface atomic electrons usually can be neglected. As shown in paper I, at such separations the intercluster potentials are less than 10^{-13} erg and therefore sufficiently weak that little or no perturbation to the cluster structure will occur (paper I showed cluster binding energies greater than 2×10^{-12} erg). Thus, the relatively simple induced-fluctuation-type force (van der Waals) is adequate for collision-frequency calculations independently of other reaction or accommodation considerations.

Collision rates have been calculated for clusters in two fixed relative orientations. In this manner, the angular variability of the interactions is suppressed, permitting the rates to be calculated for spheres. These calculations showed that the considerable differences in center-of-mass separations at contact (or hard-sphere radii in a given orientation) are largely compensated by the differences in the long-range interaction potentials that are also orientation dependent with the result that the two rates differ by less than 1%. By computing a rotationally averaged potential energy and treating the clusters as true spheres whose diameters are those of the spheres circumscribed about the clusters, the rates were shown to agree closely with the orientation-dependent rates.

Computing the collision frequencies of free-molecular aerosols is relatively well defined for spherical particles and serves as a "macroscopic limit" for cluster-collision frequencies. To determine the convergence of the cluster rates to the aerosol rates, comparisons were made for the cluster types and collision approaches of these papers. The cases of 13-, 33-, and 55-molecule clusters examined here showed that while the smallest cluster-collision rate differed from the macroscopic by about 50%, the rates for the larger two cluster pairs decreased to less than a 15% difference from the rates for spheres. Since the sum-over-pair interaction energy with the Lifshitz-Hamaker constant used in these studies represents only the upper limit on the magnitude of the interaction energy, the prospects are good for improved agreement with the use of the complete expression for the Lifshitz–van der Waals interaction energy.[16]

ACKNOWLEDGMENTS

This work was supported by the U.S. Department of Energy under Grant No. DE-FG05-87ER60550.

---

*Author to whom correspondence should be addressed.

[1] F. F. Abraham, *Homogeneous Nucleation Theory* (Academic, New York, 1974).

[2] J. M. Soler, N. Carcía, O. Echt, K. Sattler, and E. Recknagel, Phys. Rev. Lett. **49**, 1857 (1982).

[3] J. G. Gay and B. Berne, J. Colloid Interface Sci. **109**, 90 (1986).

[4] A. S. Amadon and W. H. Marlow, preceding paper, Phys. Rev. A **43**, 5483 (1991).

[5] This assertion is predicated on the absence of "fast, exoergic" reactions such as the "harpoon mechanism" between the col-

liding clusters (see Ref. 6).

[6] R. D. Levine and R. B. Bernstein, *Molecular Reaction Dynamics and Chemical Reactivity* (Oxford University Press, New York, 1987), p. 185. In the terminology of chemical reaction kinetics such as treated in this reference, the calculation of this paper treats the rate of passage of reactants though the "transition state" which is this limit.

[7] W. H. Marlow, J. Chem. Phys. **73**, 6284 (1980).

[8] A. S. Amadon and W. H. Marlow (unpublished).

[9] J. Mahanty and B. W. Ninham, *Dispersion Forces* (Academic, New York, 1976).

[10] W. H. Marlow, J. Chem. Phys. **73**, 6288 (1980).

[11] N. A. Fuchs and A. Sutugin, J. Colloid Sci. **20**, 442 (1965).

[12] M. G. Sceats, J. Chem. Phys. **84**, 5206 (1986).

[13] M. G. Sceats, J. Colloid Interface Sci. **129**, 105 (1989).

[14] S. C. Graham and J. B. Homer, Discuss. Faraday Soc. **7**, 85 (1973).

[15] W. H. Marlow, Surf. Sci. **106**, 529 (1981).

[16] D. Langbein, J. Phys. Chem. Solids **32**, 1657 (1971).